Indian Journal of Biochemistry & Biophysics
Vol. 62, September 2025, pp. 978-989
DOI: 10.56042/ijbb.v62i9.15726

Virtual screening study to identify GSK-3β inhibitors: A combined ligand-based and structure-based drug discovery approach

Anuj Kumar Mishra[1], Ravi Singh[2], Ankit Ganeshpurkar[3], Gireesh Kumar Singh[4], Pankaj Agrawal[5]
Sushil Kumar Singh[2] & Ravi Bhushan Singh[5]*

[1]SHEAT College of Pharmacy, Gahani, Ayar, Varanasi-221 210, Uttar Pradesh, India

[2]Pharmaceutical Chemistry Research Laboratory, Department of Pharmaceutical Engineering & Technology, Indian Institute of Technology (Banaras Hindu University) , Varanasi-221 005, Uttar Pradesh, India

[3]Department of Pharmaceutical Sciences, Dr. Harisingh Gour Vishwavidyalaya (A Central University) , Sagar-470 003, Madhya Pradesh, India

[4]Department of Pharmacy, School of Health Science, Central University of South Bihar, Panchanpur, Tekari Road, Gaya-824 236, Bihar, India

[5]Center of Excellence in Pharmaceutical Sciences, Guru Gobind Singh Indraprastha University, Dwarka, New Delhi-110 078, Delhi, India

Received 14 December 2024; *revised 07 July 2025*

Alzheimer's disease (AD) is a prevalent neurodegenerative disorder affecting millions worldwide. While its aetiology is complex, a central role is attributed to the dysregulation of amyloid-beta (Aβ) protein homeostasis. Emerging evidence supports the involvement of glycogen synthase kinase-3β (GSK-3β) in AD pathogenesis through its influence on Aβ production and accumulation. Inhibiting GSK-3β is considered a promising therapeutic strategy to mitigate Aβ-related neurotoxicity. This study employed ligand-based drug design and computational modelling to identify novel GSK-3β inhibitors. Leveraging the pharmacophore of the known inhibitor CX-4945, a virtual screening campaign was conducted against the Molport database. The resulting hits were subjected to rigorous filtering based on drug-likeness and PAINS criteria. Subsequent docking and molecular dynamics simulations identified MolPort-002-524-637 and MolPort-006-387-505 as promising candidates. These compounds exhibited superior binding affinities compared to CX-4945 and displayed favourable *in silico* ADME/Tox properties.

Keywords: Alzheimer's disease, Drug discovery, GSK-3β inhibitors, HTVS, Molecular dynamics simulations

Alzheimer's disease (AD) has been classified as a major global public health challenge by the World Health Organisation. Despite significant progress in understanding AD pathogenesis since its initial description by Alois Alzheimer in 1907, effective disease-modifying therapies remain elusive[1,2]. AD stands as a prominent global neurodegenerative ailment and ranks as the sixth leading contributor to mortality in the United States. Its intricacies are profound, and the pharmaceutical interventions accessible presently do not offer a complete remedy[3]. Numerous studies have demonstrated promising outcomes in cases where the accumulation of amyloid-beta (Aβ) , a hallmark of AD, was inhibited using chemical or biological means. These interventions resulted in significant enhancements in both symptoms and biomarkers associated with the disease[4]. Ongoing clinical trials exploring potential treatments for AD include various drug categories such as Aβ anti-aggregates, Aβ transport enhancers, Aβ vaccines, and passive immunisation therapies targeting Aβ. Among these, notable candidates like injectable antibodies (such as aducanumab, gantenerumab, and BAN2401) and an oral agent called ALZ-801 are showing considerable potential by specifically addressing Aβ deposition[5].

*Correspondence:
Phone: +91-9696353944 (Mob)
E-mail: ravibhushan@ipu.ac.in

Abbreviations: AD, Alzheimer's disease; APP, amyloid precursor protein; Aβ, Amyloid β; DSV, Discovery Studio Visualizer; GSK-3β, Glycogen Synthase-3β; HA, Hydrogen bond acceptor; HD, Hydrogen bond donor; HTVS, High-throughput virtual screening; HY, Hydrophobic group; LGA, Lamarckian genetic algorithm; LTP, Long term potentiation, MD, Molecular Dynamics; MW, Molecular weight; NFT, Neurofibrillary tangle; PAINS, Pan-assay interference compounds; PDB, Protein data bank; RB, Rotatable bond; SP, Standard Precision; TPSA, Topological polar surface area; XP, Extra precision

Glycogen Synthase kinase 3 beta (GSK-3β) is a serine/threonine protein kinase characterised by a bi-lobed structure. The N-terminal lobe is responsible for ATP binding, while the C-terminal lobe houses the activation loop crucial for kinase activity[6]. A tyrosine residue within the C-terminal lobe is essential for full enzyme activity. The structure of GSK-3β reveals a unique mechanism of phosphorylation, requiring a primed serine or threonine residue on the substrate for optimal catalysis. GSK-3β plays a crucial role in memory formation and consolidation. It is involved in regulating synaptic plasticity, a cellular process essential for learning and memory. While moderate levels of GSK-3β activity are necessary for these cognitive functions, excessive or aberrant activity has been linked to memory impairment. The kinase is involved in the phosphorylation of key proteins involved in synaptic remodelling and long-term potentiation (LTP) , a cellular mechanism underlying memory formation[7,8].

GSK-3β plays a pivotal role in the pathogenesis of AD. Its dysregulation is intricately linked to the core pathological hallmarks of the disease, including the formation of Aβ plaques and neurofibrillary tangles (NFTs) [9]. Overactivation of GSK-3β contributes to the hyperphosphorylation of tau protein, a critical event in NFT formation. Additionally, the kinase is involved in regulating the amyloid precursor protein (APP) processing, influencing Aβ production[10]. Furthermore, GSK-3β is implicated in neuroinflammation and neuronal cell death, exacerbating AD progression. Targeting GSK-3β has emerged as a promising therapeutic strategy for AD, with the aim of attenuating its pathological effects and improving cognitive function[11,12].

GSK-3β inhibitors show promise as potential treatments for AD by reducing tau hyper–phosphorylation, decreasing Aβ production, and exerting anti-inflammatory and neuroprotective effects[8,13,14]. Structure-based pharmacophore modelling, utilising a co-crystallised ligand-protein complex, was employed to rapidly identify potential hit compounds. The integration of pharmacophore modelling with molecular dynamics (MD) simulations enhanced the predictive accuracy of the approach. This study combines pharmacophore-based virtual screening with other computational tools to discover novel GSK-3β inhibitors.

Materials and Methods

Generation of pharmacophore model

The concept of a pharmacophore underpins the rational design of novel therapeutic agents. It is defined as a collection of essential molecular features recognised by a biological target's binding site, a pharmacophore dictates a molecule's biological activity[11]. Crucially, a class of compounds can share these features, enabling them to interact with specific complementary locations on the target molecule. These features encompass the critical steric, electronic, and functional hotspots necessary for interaction with the desired pharmacological target (s) [15].

In this study, the structure of GSK-3β bound to CX-4945 (PDB ID: 7Z1F) was used (https://www.rcsb.org/structure/7Z1F) . The Pharmit server (https://pharmit.csb.pitt.edu) was utilised to analyse the observed interactions between the protein and CX-4945 (PDB ID: 7Z1F) , with the identified pharmacophoric properties serving as queries for structure-based virtual screening. Pharmacophore models were subsequently constructed based on this ligand-receptor complex information.

Virtual screening using pharmacophores

The Pharmit server (http://pharmit.csb.pitt.edu/) was used to identify potential GSK-3β inhibitors[16]. A pharmacophore model, derived from the known inhibitor CX-4945, was employed to query the MolPort small molecule database (over 693 million entries, https://www.molport.com) . During virtual screening, candidate molecules were aligned with the pharmacophore to minimize the Root Mean Square Deviation (RMSD) between their features and those in the model.

Drug-likeliness filtering and ADME prediction

Swiss ADME was employed to assess pharmacokinetics, drug-likeness, and medicinal chemistry properties of selected hit compounds. Compounds were filtered based on Lipinski's Rule of Five and BBB permeability. Compounds adhering to the Rule of Five were selected for further analysis[17, 18]. The small molecules that violated the criterion were eliminated.

Homology modelling and evaluating models

A publicly available automated modelling service called SWISS-MODEL (https://swissmodel.expasy.org) was employed for model generation. First, the protein

sequence of interest was retrieved from UniProt using its accession code P49841. This sequence was then used to identify a suitable template structure (PDB ID: 7Z1F) from the Protein Data Bank. Finally, the user template mode of SWISS-MODEL was used to build the homology model. The quality of the generated model was subsequently evaluated using established tools like GMQE, QMEAN, and MolProbity[19-22].

Preparation of protein

The X-ray crystal structure of the GSK-3β protein complexed with the potent inhibitor CX-4945 (IC_{50} = 5 nM) was retrieved from the RCSB PDB (PDB ID: 7Z1F) . The protein structure was prepared using AutoDock Tools 1.5.6 by adding hydrogen atoms, assigning atom types, and calculating charges. Water molecules, bound ligands, and ions were removed, and the protein structure was converted into the AutoDock-compatible PDBQT format[23].

Preparation of ligand

To optimise molecular geometry and remove steric clashes, energy minimisation was performed on the selected compounds using RD kit. The energy-minimised ligands were subsequently converted into the PDBQT format for compatibility with MGL Tools-1.5.6[24].

Grid formation and confirmation

The PLIP web server (http://plip.biotec.tu-dresden.de/plip-web/plip/index) was used to identify the key amino acid residues forming the active site of the GSK-3β protein (validated using the interaction profile of CX-4945, Fig. 1) [25]. These residues were then used to define a grid box around the active site for docking simulations. AutoGrid 4.0 generated grid maps suitable for calculating interaction energies between the ligands and different atom types within the protein[26]. The grid box size was optimized for the study (64×56×46 points) with a grid spacing of 0.375 Å. The centre of the grid was positioned at 26.08, -15.046, 7.114 based on the active site location.

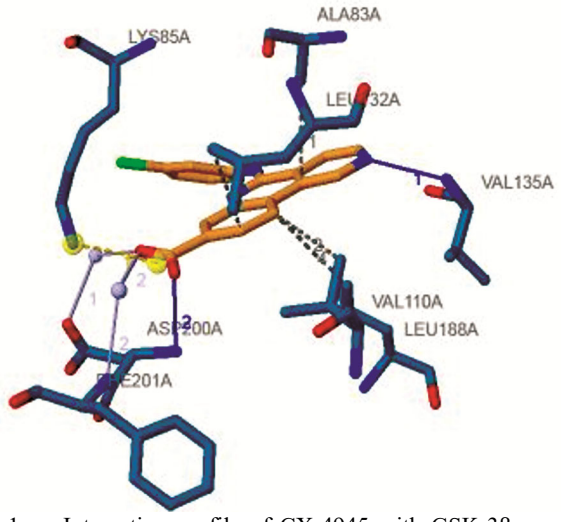

Fig. 1 — Interaction profile of CX-4945 with GSK-3β receptor (PDB id-7Z1F) displaying various interactions

Molecular docking

Docking studies were conducted in three stages high-throughput virtual screening (HTVS) , standard precision (SP) and extra precision (XP) using AutoDock 4.2.6 with the Lamarckian genetic algorithm (LGA) . The identified compounds were docked against GSK-3β, followed by post-docking analysis and visualization using Discovery Studio Visualizer 2021[24,27].

Estimation of toxicity and ADME using *in silico*

The identified lead compounds were subjected to ADME/Tox evaluation. This step, crucial for early drug development, assessed the absorption, distribution, metabolism, excretion, and potential toxicity of the compounds using SwissADME (http://www.swissadme.ch) and PreADMET (https://preadmet.bmdrc.kr/toxicity) servers[28].

Study of molecular dynamics

Compounds exhibiting favorable ADME properties were subjected to MD simulations using AMBER. The protein-ligand complexes (7Z1F-MolPort-002-524-637 and 7Z1F-MolPort-006-387-505) were solvated in a TIP3P water box and neutralized with counterions. MD simulations (200 ns) were performed under NPT conditions at 310 K using previously reported protocol[29,30]. The resulting trajectories were analyzed for RMSD, RMSF, and protein-ligand interactions to understand the dynamic behavior of the complexes.

Results and Discussion

Pharmacophore-based virtual screening

GSK-3β is identified as a potential drug target for AD. The co-crystallized small-molecule GSK-3β inhibitor CX-4945 with GSK-3β has demonstrated a K_i value of 5 nM. The pdb id 7Z1F containing CX-4945 was used for pharmacophore model development. The crystal was well resolved using

X-ray diffraction with a resolution of 3.0 Å. The ligands present in the crystal structure was used to map the pharmacophoric characteristics, including the hydrophobic group (HY) , aromatic ring (A) , hydrogen bond acceptor (HA) , and hydrogen bond donor (HD) as shown in (Fig. 2) . The resulting pharmacophore was used to carry out virtual screening using the Pharmit server and Molport database[31,32]. The 716 ligands that were identified as a result of the screening with anm RMSD below 2 Å.

Prediction of drug likeness and ADME properties

The physicochemical characteristics and drug-likeliness properties of small compounds are crucial elements for clinical effectiveness and were analysed for the obtained hits. The chosen molecules were assessed using SwissADME, a user-friendly web application that provides free access to numerous quick and dependable models for pharmacokinetics, drug-likeliness, and therapeutic chemistry, as well as physical characteristics[33]. The hits with good drug-likeliness and ADME properties are reported in (Tables 1 & 2) . The bioavailability of the ligands was further assessed utilising filters including the Lipinski rule of 5 and blood-brain barrier (BBB) permeability. Further study was performed on the ligands that displayed no violations of the applied filters[34].

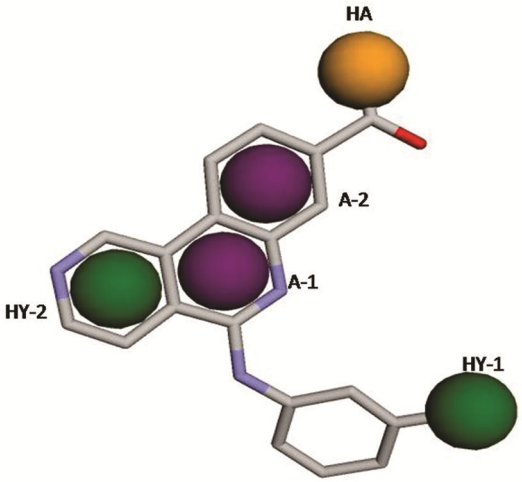

Fig. 2 — 3D Pharmacophoric features generated on Pharmitserver Pharmacophore model of CX-4945 used for virtual screening (A-1: Aromatic; HY-1: Hydrophobic; HA: Hydrogen acceptor-bond; HY-2: Hydrophobic, A-2: Aromatic)

Homology modelling and model evaluation

The 3D structure of the aligned protein after homology modelling has been represented in (Fig. 3) . The homology model's quality assessment involved an evaluation through GMQE, QMEAN and Ramachandran plots. The GMQE score was determined to be 0.81, while the QMEAN Z-score for the model was -1.23. A summary of the validation results for the modelled protein can be represented in (Fig. 3) . Ramachandran plot was obtained from web servers, *i.e*. MolProbity, and the results are summarised in a (Table 3) . The Ramachandran plot analysis showed just one residue in the disallowed region (Fig. 3) .

Molecular docking study

CX-4945 and the 155 shortlisted ligands underwent docking with the target protein. HTVS was employed as an initial filtering method using AutoDock 4.2.6[35]. Subsequently, more accurate docking poses were generated using AutoDock 4.2.6 and the LGA for both SP and XP docking[36].

Table 1 — Predicted physicochemical, gastrointestinal absorption, and blood–brain barrier permeability profiles of selected small-molecule candidates. The table summarizes key molecular descriptors including molecular weight (MW) , number of rotatable bonds (RB) , hydrogen bond acceptors (HBA) , hydrogen bond donors (HBD) , and topological polar surface area (TPSA) . Additionally, predicted gastrointestinal (GI) absorption and blood–brain barrier (BBB) permeability are provided to assess the compounds' oral bioavailability and central nervous system (CNS) penetration potential

Molecule	MW	RB	HBA	HBD	TPSA	GI absorption	BBB permeant
MolPort-023-309-886	372.21	3	3	1	59.31	High	Yes
MolPort-000-521-396	327.76	3	3	1	59.31	High	Yes
MolPort-000-663-655	316.44	8	4	1	45.59	High	Yes
MolPort-002-524-637	317.42	8	4	1	53.68	High	Yes
MolPort-006-709-114	266.68	4	5	0	61.31	High	Yes
MolPort-003-790-241	295.76	6	4	1	56.27	High	Yes
MolPort-010-795-548	445.48	7	6	1	63.99	High	No
MolPort-039-033-505	444.43	5	5	1	68.4	High	No
MolPort-045-958-668	406.52	9	3	2	68.18	High	Yes
MolPort-006-387-505	396.91	3	3	0	36.69	High	Yes

Table 2 —*In silico* prediction of cytochrome P450 (CYP450) enzyme inhibition profiles for selected compounds

Molecule	CYP2C19 inhibitor	CYP2C9 inhibitor	CYP2D6 inhibitor	CYP3A4 inhibitor
MolPort-023-309-886	Yes	Yes	No	Yes
MolPort-000-521-396	Yes	Yes	No	Yes
MolPort-000-663-655	No	No	Yes	No
MolPort-002-524-637	Yes	No	Yes	No
MolPort-006-709-114	Yes	Yes	No	No
MolPort-003-790-241	Yes	Yes	Yes	No
MolPort-010-795-548	Yes	Yes	No	Yes
MolPort-039-033-505	Yes	Yes	No	Yes
MolPort-045-958-668	Yes	Yes	Yes	Yes
MolPort-006-387-505	Yes	Yes	Yes	Yes

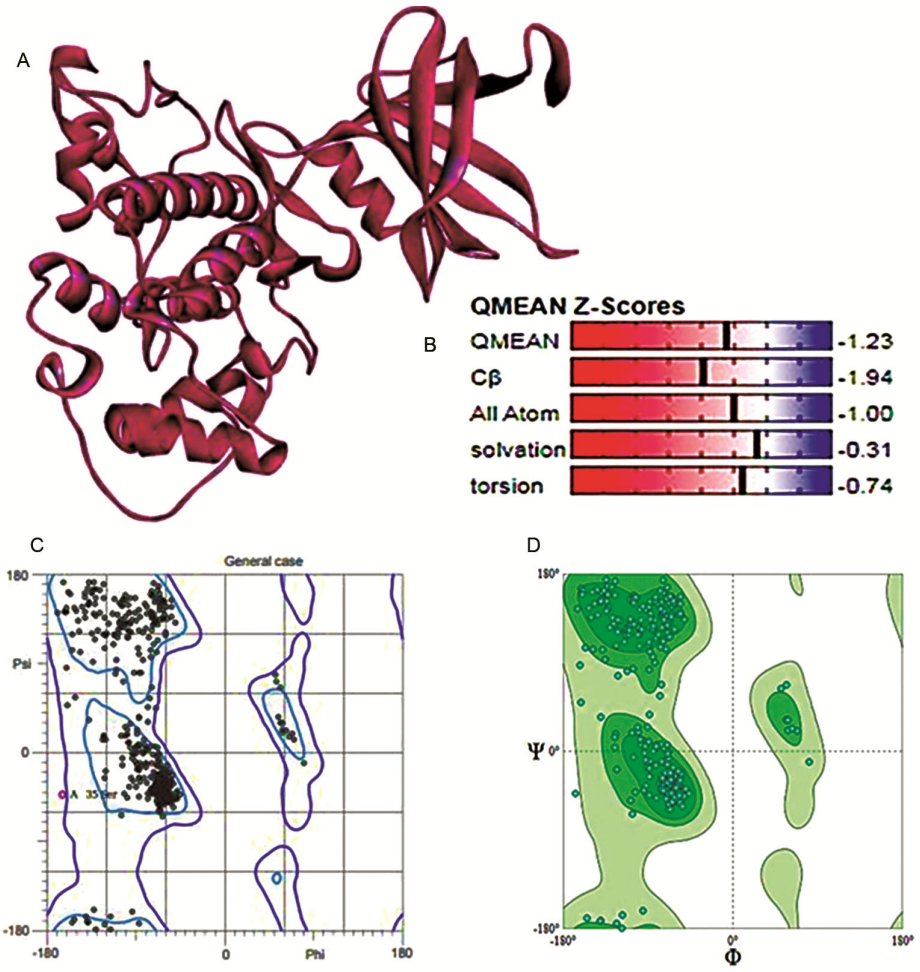

Fig. 3 — (A) 3D-structure of protein GSK-3β (7Z1F) after homology modelling; (B) QMEAN and its constituent parts into the created model; and (C & D) Ramachandran plot of the human GSK-3β before and after the homology model was created

A library of 155 compounds was initially identified through HTVS. Fifty of these compounds were subsequently subjected to SP docking. Following this, a more rigorous XP docking analysis was performed on the top 25 compounds from the SP docking results, ultimately yielding a set of 10 lead compounds (Table 4) . DSV was used for the post-docking analysis and visualization. MolPort-002-524-637 exhibited conventional hydrogen bonding interactions with Lys85 of GSK-3β. Additionally, the ligand formed weaker π-alkyl contacts with Ala83 and Leu188, as well as a π-sulfur

Table 3 — Ramachandran parameter for the developed homology model using Mol Probity

	Residues for in allowed region (%)	Residues for in outlier region (%)
Mol Probity	94.57	0.29

Table 4 — LGA specifications for docking with Standard and Extra Precision

	Standard precision (SP)	Extra precision (XP)
Number of compounds applied to docking	50	25
Result obtained	25	10
Number of GA runs	50	100
GA Population size	150	150
Crossover frequency	0.8	0.8
Rate of Gene mutation	0.02	0.02
Number of generations at its maximum	27000	27000
Maximum number of evaluations	2500000	2500000

interaction with Cys199. MolPort-006-387-505 formed a standard hydrogen bond with Asp200. Additionally, π-alkyl interactions were observed between the ligand and both Ala83 and Lys85 residues[37] (Fig. 4) .

Toxicity risk assessment

Due to the high GI and BBB permeability of eight out of ten compounds, further toxicity tests on all of these substances were carried out on the PreADMET server (https://preadmet.webservice.bmdrc.org/toxicity) [38]. Toxicity assessment included AMES toxicity, carcinogenicity against rat and mouse models, hERG inhibition, and the assessment to find hits with minimal toxicity. The model constructed through toxicological information of rats and mice collected from the National Toxicology Programme and US-FDA forms the basis for the PreADMET prediction for carcinogenicity. Two substances, namely MolPort-002-524-637 and MolPort-006-387-505, were discovered not to be oncogenic in the Ames test. These forecasts and the stage 3 docking were used to select these two compounds for additional molecular docking. The toxicity forecasts for a few chemicals are summarised in (Table 5) .

Molecular dynamics simulation study

MD simulations spanning 100 nanoseconds were conducted to assess the stability and conformational flexibility of ligand molecules complexed with GSK-3β enzymes. MD simulations are a computational technique that provides atomistic-level insights into the dynamics and interactions within complex systems. By monitoring molecular conformations, solvation, protein structural fluctuations, and ligand-protein interactions, MD simulations offer valuable information regarding the behaviour of biomolecular complexes[39]. The Desmond module within the Schrodinger suite was employed for the MD simulations[40].

This study focused on two GSK-3β protein-ligand complexes: MolPort-002-524-637 and MolPort-006-387-505. The complexes were solvated in a cubic TIP3P water box with a cutoff distance of 4 Å. Counterions were added to neutralise the system's net charge. The MD production phase was executed under constant pressure and temperature (NPT) conditions at 310 K for 100 ns. Subsequent analysis of the generated MD trajectory encompassed bond formation, residue-ligand contact frequency, root mean square deviation (RMSD) of protein-ligand complexes, protein root mean square fluctuation (RMSF) , and ligand RMSF. To ensure system equilibration prior to production simulations, the mean RMSD of temperature, peptide backbone, and density over time was monitored.

RMSD

RMSD defines the overall difference between two molecules or groups of atoms in terms of their structure. In MD, it expresses the extent to which a molecule samples from the reference structure in time. The variability of RMSD shows that a small stable value shows the structural stability of the protein, whereas a large variation indicates conformational change. RMSD is applied for the measurement of protein stability, ligand binding, and achieving the state of equilibrium of a system. Though it has some drawbacks that include being sensitive to the first alignment and being incapable of modelling large-distinct conformational movements. The mean RMSDs of GSK-3β complexed with MolPort-002-524-637 and MolPort-006-387-505 were found to be 2.879 ± 0.251 and 2.785 ± 0.235 Å, respectively. The RMSD between 1 – 3 Å for globular proteins indicate stability. As MD simulation progressed, a stable RMSD was observed, reflecting the overall stability of the system. The RMSD between 1 – 3 Å for globular proteins indicate stability.

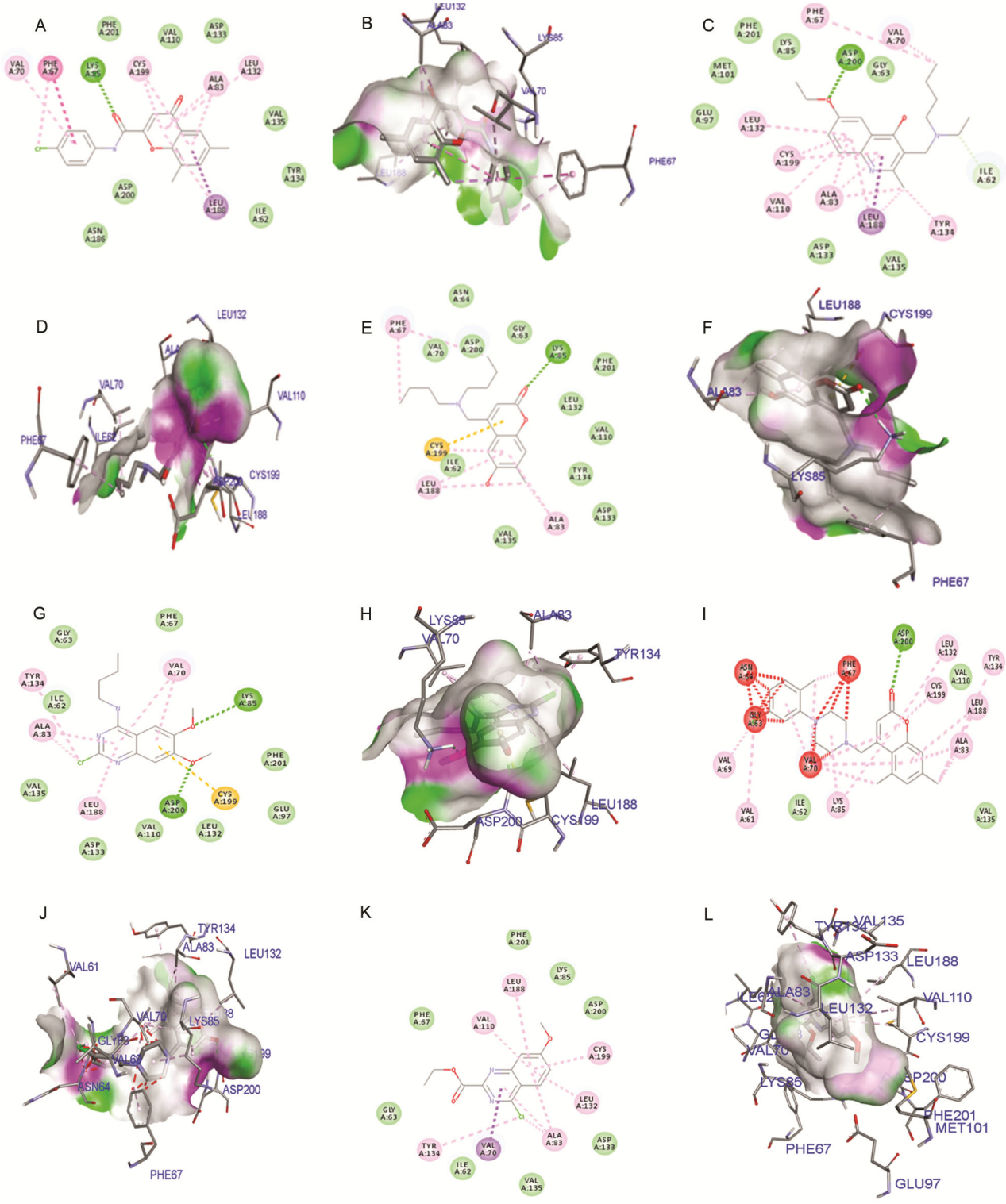

Fig. 4 — 2D & 3D interaction diagram of (A & B) MolPort-000-521-396; (C & D) MolPort-000-663-655; (E & F) MolPort-002-524-637; (G & H) MolPort-003-790-241; (I & J) MolPort-006-387-505; (K & L) MolPort-006-709-114; (M & N) MolPort-010-795-548; (O & P) MolPort-023-309-886; (Q & R) MolPort-039-033-505; and (S & T) MolPort-045-958-668 (*Contd.*)

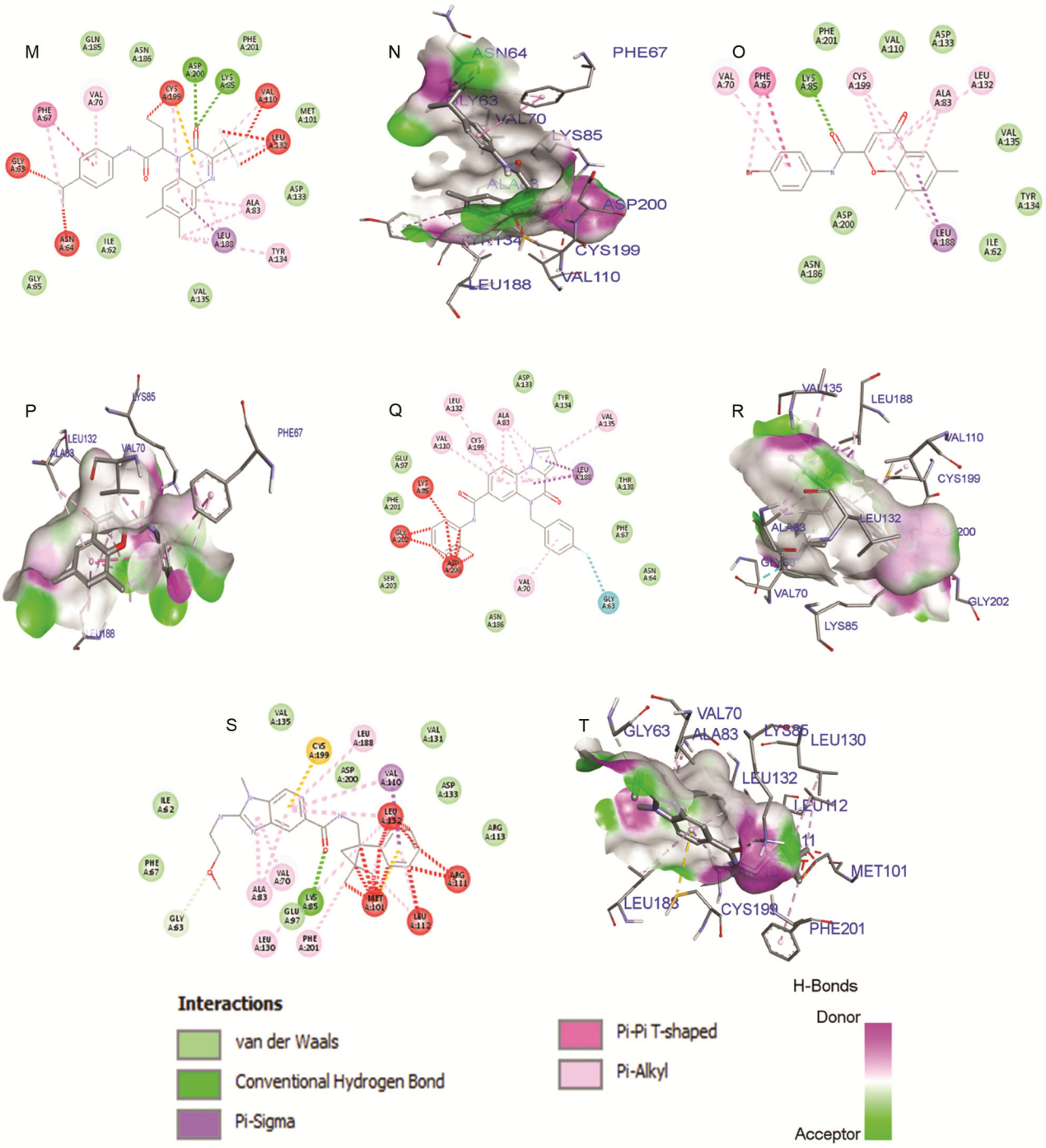

Fig. 4 — 2D & 3D interaction diagram of (A & B) MolPort-000-521-396; (C & D) MolPort-000-663-655; (E & F) MolPort-002-524-637; (G & H) MolPort-003-790-241; (I & J) MolPort-006-387-505; (K & L) MolPort-006-709-114; (M & N) MolPort-010-795-548; (O & P) MolPort-023-309-886; (Q & R) MolPort-039-033-505; and (S & T) MolPort-045-958-668

The mean RMSDs of MolPort-002-524-637 and MolPort-006-387-505 were found to be 1.513 ± 0.483 and 1.339 ± 0.243 Å, respectively. The RMSD indicated that the ligands were stable in the cavity (Fig. 5) .

RMSF

RMSF is a crucial metric which quantifies the average deviation of atomic positions from their mean positions over time. It serves as a powerful tool to explore the flexibility and dynamics of a molecule,

Table 5 — Predicts the *in silico* toxicity profile for substances from pre-ADMET

Compound Id	Ames test	Carcino Rat	hERG inhibition	TA100_10RLI	TA1535_NA
MolPort-000-521-396	Mutagen	Negative	Medium Risk	Positive	Negative
MolPort-000-663-655	Mutagen	Positive	Low Risk	Negative	Negative
MolPort-002-524-637	Non-Mutagen	Negative	Low Risk	Negative	Negative
MolPort-003-790-241	Mutagen	Negative	Low Risk	Negative	Positive
MolPort-006-387-505	Non-Mutagen	Negative	Medium Risk	Negative	Negative
MolPort-006-709-114	Mutagen	Negative	Low Risk	Positive	Positive
MolPort-010-795-548	Mutagen	Positive	Medium Risk	Positive	Negative
MolPort-023-309-886	Mutagen	Positive	Medium Risk	Positive	Negative
MolPort-039-033-505	Mutagen	Negative	Medium Risk	Negative	Negative
MolPort-045-958-668	Mutagen	Negative	Medium Risk	Negative	Negative

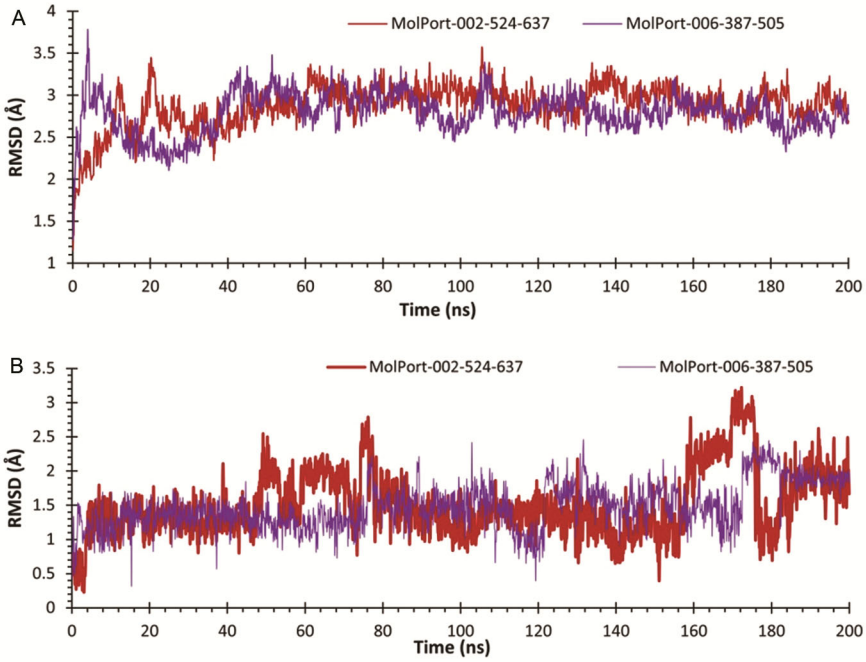

Fig. 5 — (A) RMSD plots of GSK-3β protein complexed with MolPort-002-524-637 and MolPort-006-387-505; and (B) RMSD plots of MolPort-002-524-637 and MolPort-006-387-505 bound to GSK-3β

particularly proteins. High RMSF value indicates flexible domains, potential binding sites, and functionally important regions in the protein structure. Both molecular complexes exhibited higher fluctuations in specific residue regions, with GSK-3β -MolPort-002-524-637 complex showing greater fluctuations in the early residue numbers, i.e. up to around residue 40, compared to GSK-3β -MolPort-006-387-505. Significant differences are observed at residues 28-33, 37-50, and 91-94, where GSK-3β -MolPort-002-524-637 has notably higher RMSF values. Both ligands have stabilised regions with low RMSF values in the residue ranges 37-46 and 100-170. High fluctuations are observed in both ligands at residues 66-70, 146-150, and 207-210. The RMSF values for MolPort-002-524-637 and MolPort-006-387-505 reveal distinct patterns in atomic fluctuations. MolPort-002-524-637 demonstrates lower fluctuations in the initial atoms (1-10) compared to MolPort-006-387-505. However, significant deviations are observed for MolPort-002-524-637 between atoms 14-20 and 23-50, with notably higher fluctuations, especially at atoms 19, 24, 37-39, 46, and 48-50, indicating greater instability in these regions. Conversely, MolPort-006-387-505 maintains more consistent, albeit higher, fluctuation values across most atoms, suggesting a different stability profile. The peak fluctuations for MolPort-

002-524-637 are observed at atoms 19 and 37-39, while MolPort-006-387-505 shows peak values around atoms 31-33 and 39 (Fig. 6) .

Radius of Gyration

The radius of gyration (RoG) analysis in simulations provides insights into the compactness and structural stability of the molecules. The mean RoGs of GSK-3β complexed with MolPort-002-524-637 and MolPort-006-387-505 were found to be 22.004 ± 0.111 and 21.978 ± 0.192 Å, respectively. There was no unfolding observed for both complexes, indicating stability. In the case of ligands, the mean RoGs were found to be 3.695 ± 0.129 and 4.625 ± 0.148 Å, respectively, for MolPort-002-524-637 and MolPort-006-387-505 (Fig. 7) .

Solvent accessible surface area (SASA)

SASA is a measure of the molecular surface that is exposed to a solvent. In the context of biomolecules,

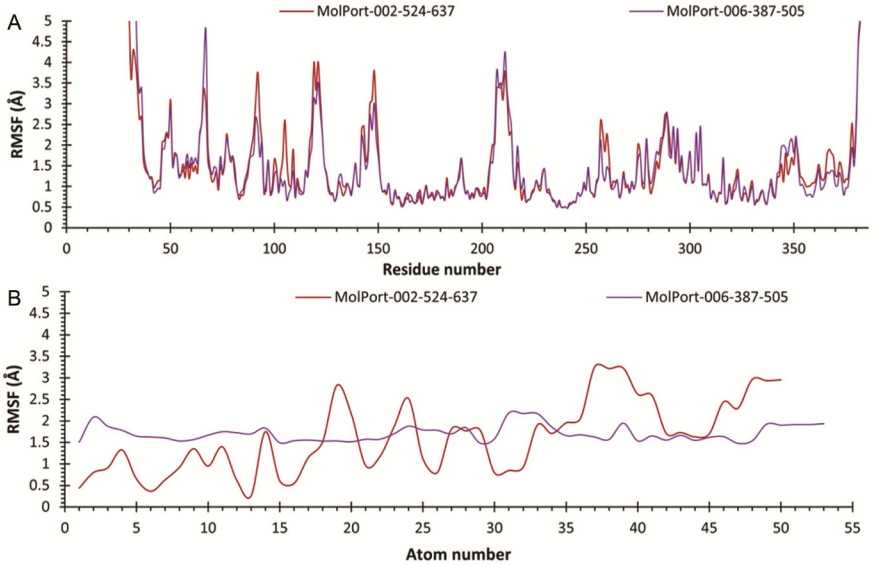

Fig. 6 — (A) RMSF plots of GSK-3β protein complexed with MolPort-002-524-637 and MolPort-006-387-505; and (B) RMSF plots of MolPort-002-524-637 and MolPort-006-387-505

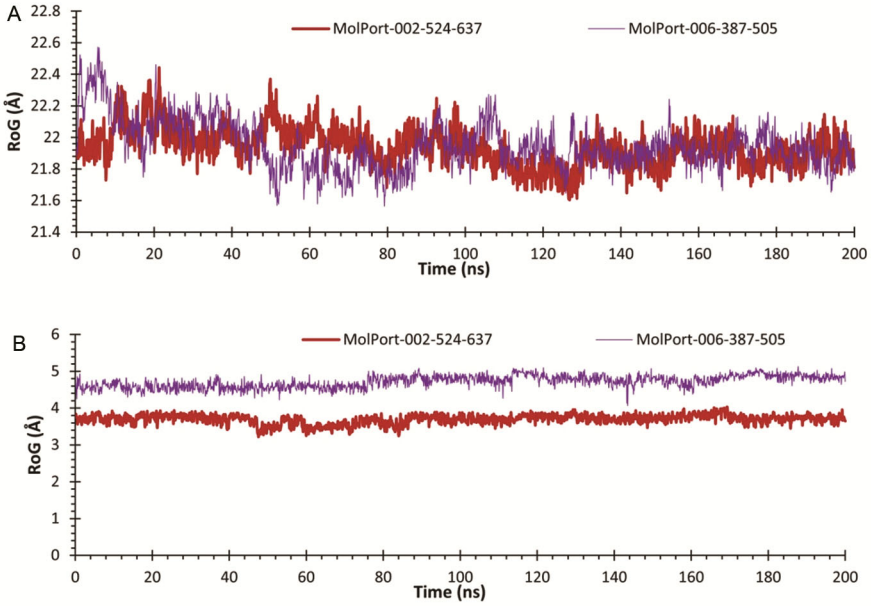

Fig. 7 — (A) RoG of GSK-3β protein complexed with MolPort-002-524-637 and MolPort-006-387-505; and (B) RoG plots of MolPort-002-524-637 and MolPort-006-387-505

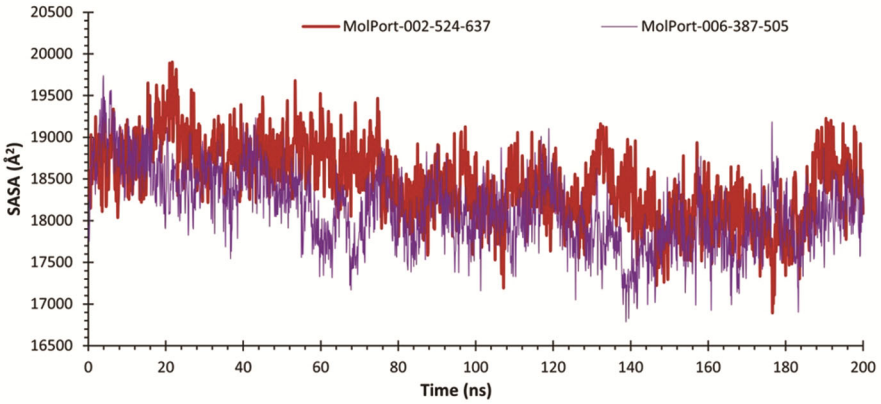

Fig. 8 — (A) SASA of GSK-3β protein complexed with MolPort-002-524-637 and MolPort-006-387-505; and (B) SASA plots of MolPort-002-524-637 and MolPort-006-387-505

it quantifies the portion of the molecule that is accessible to water molecules. The mean SASA of GSK-3β complexed with MolPort-002-524-637 and MolPort-006-387-505 were found to be 18453.107 ± 453.297 and 18338.942 ± 434.409 Å^2, respectively. Protein folding and the energetics are revealed by changes in SASA. SASA of binding sites can therefore aid in the determination of ligand binding affinities as well as the dynamics of ligand binding to the protein target. In the present study, no significant SASA change was observed (Fig. 8) .

Conclusion

This study employed a multi-faceted computational approach to identify potential GSK-3β inhibitors for the treatment of AD. By integrating pharmacophore modelling, virtual screening, molecular docking, and molecular dynamics simulations, we successfully identified two promising compounds, MolPort-002-524-637 and MolPort-006-387-505. These compounds exhibited favourable drug-likeliness properties, demonstrated promising binding interactions with GSK-3β, and displayed acceptable toxicity profiles. While these findings are encouraging, further experimental validation is necessary to confirm their efficacy and safety as therapeutic agents. The identification of these compounds represents a significant step towards developing novel treatments for AD and underscores the potential of computational drug discovery in accelerating the drug development process.

Acknowledgement

We thank all our authors for their valuable suggestions and support. Authors are also thankful to the support and the resources provided by the 'PARAM BRAHMA FACILITY' under the National Supercomputing Mission, Government of India at the IISER, Pune, are gratefully acknowledged. We would also like to acknowledge the computational support received from Centre for Computing and Information Services (CCIS) , Indian Institute of Technology (BHU) , Varanasi.

Conflicts of interest

All authors declare no conflicts of interest.

References

1 DriscollI & TroncosoJ, Asymptomatic Alzheimer's disease: a prodrome or a state of resilience?.*Curr Alzheimer Res*, 8 (2011) 330.
2 Chew SY & Than LTL, Vulvovaginal candidosis: contemporary challenges and the future of prophylactic and therapeutic approaches. *Mycoses*, 59 (2016) 262.
3 Rivera VI, How Traditional Definitions of Autonomy Impair Decision-making in Spinal Muscular Atrophy and Alzheimer Disease. *Temple University* (2019) 1.
4 Bazzari FH & Bazzari AH, BACE1 Inhibitors for Alzheimer's Disease: The Past, Present and Any Future? *Molecules*, 27 (2022) 8823.
5 Tolar M, Hey J, Power A & Abushakra S, Neurotoxic soluble amyloid oligomers drive Alzheimer's pathogenesis and represent a clinically validated target for slowing disease progression. *Int J Mol Sci*, 22 (2021) 6355.
6 Doble BW & Woodgett JR, GSK-3: tricks of the trade for a multi-tasking kinase. *J Cell Sci*, 116 (2003) 1175.
7 HarwoodAJ, Regulation of GSK-3: a cellular multiprocessor. *Cell*,105 (2021) 821.
8 Kaidanovich-Beilin O & Woodgett JR, GSK-3: functional insights from cell biology and animal models. *Front Mol Neurosci*, 4 (2011) 40.
9 Takashima A, GSK-3 is essential in the pathogenesis of Alzheimer's disease. *J Alzheimers Dis*, 9 (2006) 309.
10 Hu S, Begum AN, Jones MR, Oh MS, Beech WK, Beech BH, Yang F, Chen P, Ubeda OJ, Kim PC & Davies P, GSK3 inhibitors show benefits in an Alzheimer's disease (AD) model of neurodegeneration but adverse effects in control animals. *Neurobiol Dis*, 33 (2009) 193.

11 Mandlik DS & Mandlik SK, Therapeutic implications of glycogen synthase kinase-3β in Alzheimer's disease: a novel therapeutic target. *Int J Neurosci*, 134 (2024) 303.

12 Gandini A, Bartolini M, Tedesco D, Martinez-Gonzalez L, Roca C, Campillo NE, Zaldivar-Diez J, Perez C, Zuccheri G, Miti A & Feoli, A, Tau-centric multitarget approach for Alzheimer's disease: development of first-in-class dual glycogen synthase kinase 3β and tau-aggregation inhibitors. *J Med Chem*, 61 (2018) 7640.

13 Martinez A. & PerezDI, GSK-3 inhibitors: a ray of hope for the treatment of Alzheimer's disease? *J Alzheimers Dis*, 15 (2008) 181.

14 Takahashi-Yanaga F, Activator or inhibitor? GSK-3 as a new drug target. *Biochem Pharmacol*, 86 (2013) 191.

15 Gao Q, YangL & ZhuY, Pharmacophore based drug design approach as a practical process in drug discovery. *Curr Comput Aided Drug Des*, 6 (2010) 37.

16 Kumar BK, Faheem N, Sekhar KV, Ojha R, Prajapati VK, Pai A & Murugesan S, Pharmacophore based virtual screening, molecular docking, molecular dynamics and MM-GBSA approach for identification of prospective SARS-CoV-2 inhibitor from natural product databases. *J Biomol Struct Dyn*, 40 (2022) 1363.

17 BritoMA, Pharmacokinetic study with computational tools in the medicinal chemistry course. *Braz J Pharm Sci*, 47 (2011) 797.

18 Singh R, Ganeshpurkar A, Kumar D, Kumar D, Kumar A & Singh SK, Identifying potential GluN2B subunit containing N-Methyl-D-aspartate receptor inhibitors: An integrative *in silico* and molecular modeling approach. *J Biomol Struct Dyn*, 38 (2020) 2533.

19 Waterhouse A, Bertoni M, Bienert S, Studer G, Tauriello G, Gumienny R, Heer FT, de Beer TA, Rempfer C, Bordoli L & Lepore R. SWISS-MODEL: homology modelling of protein structures and complexes. *Nucleic Acids Res*, 46 (2018) W296.

20 Duvaud S, Gabella C, Lisacek F, Stockinger H, Ioannidis V & Durinx C, Expasy, the Swiss Bioinformatics Resource Portal, as designed by its users. *Nucleic Acids Res*, 49 (2021) W216.

21 Benkert P, Künzli M & Schwede T, QMEAN server for protein model quality estimation. *Nucleic Acids Res*, 37 (2009) W510.

22 Chen VB, Arendall WB, Headd JJ, Keedy DA, Immormino RM, Kapral GJ, Murray LW, Richardson JS & Richardson DC, MolProbity: all-atom structure validation for macromolecular crystallography. *Acta Crystallogr D Biol Crystallogr*, 6 (2010) 12.

23 Samdani, A. & U. Vetrivel, POAP: A GNU parallel based multithreaded pipeline of open babel and AutoDock suite for boosted high throughput virtual screening. *Comput Biol Chem*, 74 (2018) 39.

24 Swetha R, Sharma A, Singh R, Ganeshpurkar A, Kumar D, Kumar A & Singh SK, Combined ligand-based and structure-based design of PDE 9A inhibitors against Alzheimer's disease. *Mol Divers*, 26 (2022) 2877.

25 Singh R, Pokle AV, Ghosh P, Ganeshpurkar A, Swetha R, Singh SK & Kumar A, Pharmacophore-based virtual screening, molecular docking and molecular dynamics simulations study for the identification of LIM kinase-1 inhibitors. *J Biomol Struct Dyn*, 41 (2023) 6089.

26 Gujjula, K.R., Prediction and comparison of hiv-1 protease inhibitor binding energies by various molecular docking methods. *Doctoral dissertation*, (2008) 1.

27 Sousa SF, Cerqueira NMFSA, Fernandes PA & Ramos MJ, Virtual screening in drug design and development. *Comb Chem High Throughput Screen*, 13 (2010) 442.

28 Balani SK, Miwa GT, Gan LS, Wu JT & Lee FW, Strategy of utilizing *in vitro* and *in vivo* ADME tools for lead optimization and drug candidate selection. *Curr Top Med Chem*, 5 (2005) 1033.

29 Ganeshpurkar A, Singh R, Gore PG, Kumar D, Gutti G, Kumar A & Singh SK, Structure-based screening and molecular dynamics simulation studies for the identification of potential acetylcholinesterase inhibitors. *Mol Sim*, 46 (2020) 169.

30 Ganeshpurkar A, Singh R, Kumar D, Divya, Shivhare S, Kumar A & Singh SK, Computational binding study with α7 nicotinic acetylcholine receptor of Anvylic-3288: an allosteric modulator. *Mol Sim*, 46 (2020) 975.

31 Jana S, GaneshpurkarA,SinghSK, Multiple 3D-QSAR modeling, e-pharmacophore, molecular docking, and *In vitro* study to explore novel AChE inhibitors. *RSC Adv*, 8 (2018) 39477.

32 Sunseri J & KoesDR, Pharmit: interactive exploration of chemical space. *Nucleic Acids Res*, 44 (2016) W442.

33 Daina A, MichielinO, & ZoeteV, SwissADME: a free web tool to evaluate pharmacokinetics, drug-likeness and medicinal chemistry friendliness of small molecules. *Sci Rep*, 7 (2017) 42717.

34 Daoud NE, Borah P, Deb PK, Venugopala KN, Hourani W, Alzweiri M, Bardaweel SK & Tiwari V, ADMET profiling in drug discovery and development: perspectives of *in silico*, *In vitro* and integrated approaches. *CurrDrug Metab*, 22 (2021) 503.

35 Tripathi NM & BandyopadhyayA, High throughput virtual screening (HTVS) of peptide library: Technological advancement in ligand discovery. *Eur J Med Chem*, 243 (2022) 114766.

36 Umre R, Ganeshpurkar A, Ganeshpurkar A, Pandey S, Pandey V, Shrivastava A & Dubey N, *In vitro*, *in vivo* and *in silico* antiulcer activity of ferulic acid. *Futur J Pharm Sci*, 4 (2018) 248.

37 Wang C, Liu J, Luo F, Deng Z & Hu QN,Predicting target-ligand interactions using protein ligand-binding site and ligand substructures. *BMC Syst Biol*, 21 (2015) S2.

38 Lamie PF & PhiloppesJN, Design, synthesis, stereochemical determination, molecular docking study, *In silico* pre-ADMET prediction and anti-proliferative activities of indole-pyrimidine derivatives as Mcl-1 inhibitors. *Bio Chem*, 116 (2021) 105335.

39 Bronowska AK, Thermodynamics of ligand-protein interactions: implications for molecular design, in Thermodynamics-Interaction Studies-Solids, Liquids and Gases. (2011) IntechOpen.

40 Das SK, Mahanta S, Tanti B, Tag H & Hui PK, Identification of phytocompounds from Houttuynia cordata Thunb. as potential inhibitors for SARS-CoV-2 replication proteins through GC–MS/LC–MS characterization, molecular docking and molecular dynamics simulation. *Mol Div*, 26 (2022) 365.